engineering proceedings

MDPI

Proceeding Paper

Polymer/Activated Charcoal-Coated Magnetite for the Adsorptive Removal of Emerging Contaminants: Stepwise Synthesis via Two Sequential Routes †

Hebatullah H. Farghal [1,*], Marianne Nebsen [2] and Mayyada M. H. El-Sayed [1,*]

[1] Department of Chemistry, School of Sciences and Engineering, The American University in Cairo, New Cairo 11835, Egypt
[2] Analytical Chemistry Department, Faculty of Pharmacy, Cairo University, Cairo 11562, Egypt
* Correspondence: hebatullahfarghal@aucegypt.edu (H.H.F.); mayyada@aucegypt.edu (M.M.H.E.-S.)
† Presented at the 3rd International Electronic Conference on Applied Sciences, 1–15 December 2022; Available online: https://asec2022.sciforum.net/.

Abstract: Emerging contaminants pose great health risks to humans and living organisms, even when released at minute concentrations over prolonged exposure times. In this work, we fabricate nanocomposites based on activated charcoal-coated magnetite by incorporating the biopolymers of xylan or pectin into their structure. Two synthesis routes which differ in their sequential steps were investigated. It was demonstrated that the synthesis route affects the morphology, textural properties, and chemical structure of the nanocomposites, as confirmed by Scanning Electron Microscopy (SEM), Brunauer-Emmett-Teller (BET) analysis, and Fourier Transform Infra-red (FTIR) measurements, respectively. Hence, in turn, it influences the performance of the nanocomposites in their adsorptive removal for the emerging contaminants of Fluoxetine and Famotidine, whose presence in wastewater have been confirmed in several studies.

Keywords: emerging contaminant; synthesis; activated charcoal; polymer; magnetite

Citation: Farghal, H.H.; Nebsen, M.; El-Sayed, M.M.H. Polymer/Activated Charcoal-Coated Magnetite for the Adsorptive Removal of Emerging Contaminants: Stepwise Synthesis via Two Sequential Routes. *Eng. Proc.* **2023**, *31*, 42. https://doi.org/10.3390/ASEC2022-13858

Academic Editor: Nunzio Cennamo

Published: 5 December 2022

1. Introduction

Emerging contaminants are a class of organic pollutants that can be hazardous to humans and living organisms when released in water bodies at minute concentrations over prolonged exposure times. One of the main concerns of their toxicity is that there is no regulatory framework that controls their levels in the environment. Emerging contaminants are classified into several categories including pharmaceuticals and personal care products, detergents, flame retardants, pesticides, etc. [1]. This study is concerned with two pharmaceutical emerging contaminants, Fluoxetine HCl and Famotidine, which are found in surface water and in wastewater effluents of hospitals and pharmaceutical industries [2,3]. Fluoxetine (FLX) is a selective serotonin reuptake inhibitor anti-depressant. It is present in surface waters at average concentrations of 0.012 μg/L, and in effluents of wastewater treatment plants at concentrations as high as 0.540 μg/L. FLX can induce developmental abnormalities in medaka fish by about 4–5 times higher than unexposed fish [4]. Famotidine (FAM) is a histamine blocker for the treatment of ulcers. It has been detected in the effluent wastewater at concentrations of 410–5200 ng/L. Its risk quotient in algae and fish is 0.24 and <0.01, respectively [5].

One method of great importance in the eradication of emerging contaminants from wastewater is adsorption, owing to its effectiveness and operational flexibility [6]. Activated charcoal is one of the most popular adsorbents for wastewater treatment due to its high porosity and surface area which enhance the adsorption performance. However, it is difficult to handle during the treatment process and to remove from wastewater after treatment. Furthermore, it has a relatively high cost and can generate secondary pollutants [7].

Thus, we propose an environmentally friendly approach to synthesize nanocomposite adsorbents by coating activated charcoal over magnetite to enhance its separation by a magnetic field, then incorporating two naturally abundant biopolymers, xylan and pectin, into this structure to enhance its biodegradability. The synthesis takes place via two routes that differ in the order of their sequential steps, to investigate the effect of the synthesis method on the characteristics of the prepared nanocomposites and their adsorption efficiency toward FLX and FAM. There exist very few reports in the literature on the removal of these two contaminants, despite their alarming potential impacts on the environment [8,9].

2. Materials and Methods

2.1. Materials

Fluoxetine hydrochloride (FLX) of purity 100.3% (pK_a 9.8) and Famotidine (FAM) of purity 99.9% (pK_a 7.95) were cordially provided by Amoun Pharmaceutical Co., Cairo, Egypt. Activated charcoal (AC) was purchased from Adwic (part of Al-Nasr pharmaceutical chemicals company), Cairo, Egypt. Magnetic precursors of ferrous sulfate heptahydrate (98%) and anhydrous ferric chloride (97%), in addition to sodium hydroxide pellets (97%), were purchased from Alfa Aesar (Erlenbachweg, Germany) for the former and Fisher Scientific, (Loughborough, UK), for the latter two (parts of Thermo Fisher Scientific). Purified beechwood xylan (4-O-methyl glucuronoxylan of purity >95%) with 12.8% glucuronic acid was purchased from Neogen Megazyme Ltd., Bray, Ireland. Pure pectin (poly-D-galacturonic acid methyl ester with M.W. of 25,000 to 50,000 Da) with >80% galacturonic acid and >7% methoxyl content was purchased from Sisco Research Laboratories Pvt. Ltd. (SRL), Mumbai, Maharashtra, India. Hydrochloric acid (37% by vol.) was purchased from Acros Organics-Fisher Scientific, Schwerte, Germany.

2.2. Preparation of the Nanocomposites via Synthesis Route I

To prepare AC-coated magnetite using synthesis route I (CM_I), a mass of 0.5 g AC was dispersed in 30 mL distilled water and stirred. Then, 1.5 g ferrous sulfate heptahydrate and 1.75 g anhydrous ferric chloride were added and stirred for 20 min. A 30% NaOH solution was added dropwise until the solution was black, and was then stirred for 30 min. In the case of xylan-incorporated CM (XCM_I), a mass of 0.5 g xylan was dispersed in 95% ethanol and dissolved in 30 mL distilled water while heating and stirring until boiling. Once boiled, the heater was turned off and the solution was stirred for a further 10 min then left to cool. A mass of 0.5 g AC was added and stirred for 50 min. The magnetic precursors were then added as discussed above. Similarly, pectin-incorporated CM (PCM_I) was prepared by dissolving a mass of 0.5 g pectin in 30 mL distilled water for 30 min then adding 0.5 g AC while stirring for 15 min, before introducing the magnetic precursors. All the prepared nanocomposites were washed with distilled water three times and left in the air to dry.

2.3. Preparation of Nanocomposites via Synthesis Route II

To prepare AC-coated magnetite using synthesis route II (CM_{II}), masses of 1.5 g ferrous sulfate heptahydrate and 1.75 g ferric chloride anhydrous were dispersed in 30 mL distilled water for 20 min then 30%NaOH was added dropwise until the solution was black and stirred for 30 min. A mass of 0.5 g AC was then added and stirred for 15 min. For XCM_{II}, a tank containing 0.5 g xylan in 15 mL distilled water was prepared as above and added to another tank of 30 mL CM_{II}, then stirred for 50 min. Similarly, PCM_{II} was prepared separately where 0.5 g pectin was dissolved in 15 mL distilled water in a separate tank and added to the tank of 30 mL CM_{II}, and stirred for 30 min. All the prepared nanocomposites were washed three times and left in the air to dry.

2.4. Characterization of the Prepared Nanocomposites

FTIR measurements (Thermo Scientific Nicolet 380 FT-IR Spectrometer, Waltham, MA, USA) for all nanocomposites were performed to determine the existing functional groups before and after adsorption. To examine surface morphology, SEM images (Zeiss Supra 55,

Oberkochen, Germany) were taken after gold sputtering (Hummer™ 8.0, Union City, CA, USA) at 15 mA for 1 min. To determine surface areas and pore volumes, BET measurements (ASAP 2020, Micrometrics equipment, Norcross, GA, USA) were performed using nitrogen gas after degassing the samples at 40 °C for 8 h. For the determination of surface charge, DLS measurements were carried out using a Malvern Panalytical Zetasizer Nano-ZS90 (Malvern, UK).

2.5. Adsorption Experiments

Batch adsorption experiments were performed for the removal of FLX and FAM using a rotary shaker at 60 rpm for 4 h. The applied initial concentration was 25 ppm and adsorption took place at pH 7.35 using 0.67 g/L of the nanocomposite at room temperature (25 ± 2 °C). After adsorption, solutions were magnetically decanted and the supernatant was measured using a UV/VIS spectrometer (Pg instruments, T80+ spectrometer, Leicestershire, UK) at 228 and 275 nm for FLX and FAM, respectively. Obtained absorbances were substituted in the following equation:

$$\% \, Removal = \frac{\left(A_{\mathrm{i}} - A_f\right)}{A_{\mathrm{i}}} \times 100$$

where A_{i} is the absorbance before adsorption and A_f is the absorbance after adsorption [10].

2.6. Statistical Analysis

All measurements were conducted in duplicate and expressed as mean ± SD error bars. Statistical analysis was performed using the paired two-tailed Student's *t*-test at a 95% confidence level where *p*-values were calculated on Microsoft Excel 365 software.

3. Results and Discussion

3.1. Characteristics of the Prepared Nanocomposites

Surface morphologies for the nanocomposites synthesized using the two routes are shown in Figure 1. It is clear that the surfaces of XCM_I and PCM_I are rougher than that of CM_I, which appears to be relatively smooth and similar in morphology to activated carbons previously reported in literature [11]. The rough granular surfaces of XCM_I and PCM_I could be owed to the xylan or pectin polymer which probably coats the surface [12,13]. On the other hand, XCM_{II} and PCM_{II} have almost the same morphology, which is similar to that of CM_{II}, indicating that AC dominates the surface of these nanocomposites. These AC surfaces are similar to those previously reported for commercial AC and AC derived from cluster stalks [14].

The FTIR spectra of all nanocomposites (Figure 2) show bands at about 3400 and 1630 cm^{-1} which could be assigned to OH and C=O groups of carboxylic acid [15]. For BET measurements, it is evident from Table 1 that the pore volumes of CM_I and CM_{II} are comparable while the surface area of CM_I is less than that of CM_{II} by about 22%, which indicates that magnetite blocked more surface pores on CM_I. In the synthesis of CM_I, the magnetic precursors are introduced as Fe ions to the AC, and hence have high diffusivity that can allow them to access more pores and complex with the pi electrons of the hydroxyl groups of the AC [16]. In the synthesis of CM_{II}, however, the magnetic precursors are introduced to the AC as nanoparticles. This might also explain the lower FTIR peak intensity of OH shown for CM_I (Figure 2a) relative to its corresponding peak for CM_{II} (Figure 2b). This could have resulted from the involvement of the OH groups of CM_I in more complexation bonding than their counterparts of CM_{II}, and which in turn restricted their bond vibrations. Regarding the polymeric nanocomposites XCM_I, PCM_I, XCM_{II}, and PCM_{II}, they are not considerably different in their surface areas or pore volumes, but have lower areas and pore volumes than CM_I and CM_{II}. All the nanocomposites have pores that lie in the mesoporous range (2–50 nm), and they all have a negative surface charge at the working pH (Table 1).

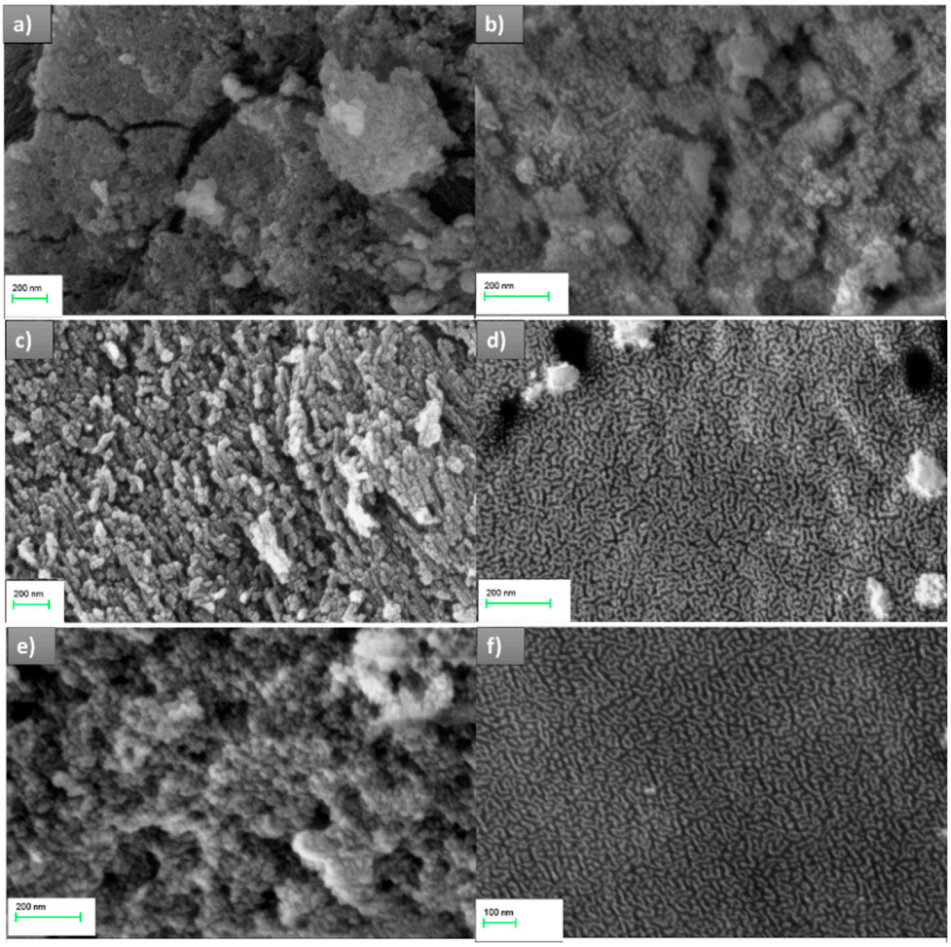

Figure 1. SEM images of (**a**) CM_I, (**b**) CM_{II}, (**c**) XCM_I, (**d**) XCM_{II}, (**e**) PCM_I, and (**f**) PCM_{II}.

Table 1. Textural properties and zeta potential of the nanocomposites.

	BET Surface Area (m^2/g)	BJH Pore Volume (cm^3/g)	Pore Size (nm)	Zeta Potential (mV)
CM_I	348.7	0.25	5.71	−39.0
CM_{II}	446.7	0.27	6.05	−29.8
XCM_I	227.1	0.16	6.07	−30.0
XCM_{II}	219.8	0.13	6.33	−27.8
PCM_I	227.5	0.16	5.56	−39.0
PCM_{II}	266.3	0.19	7.14	−37.3

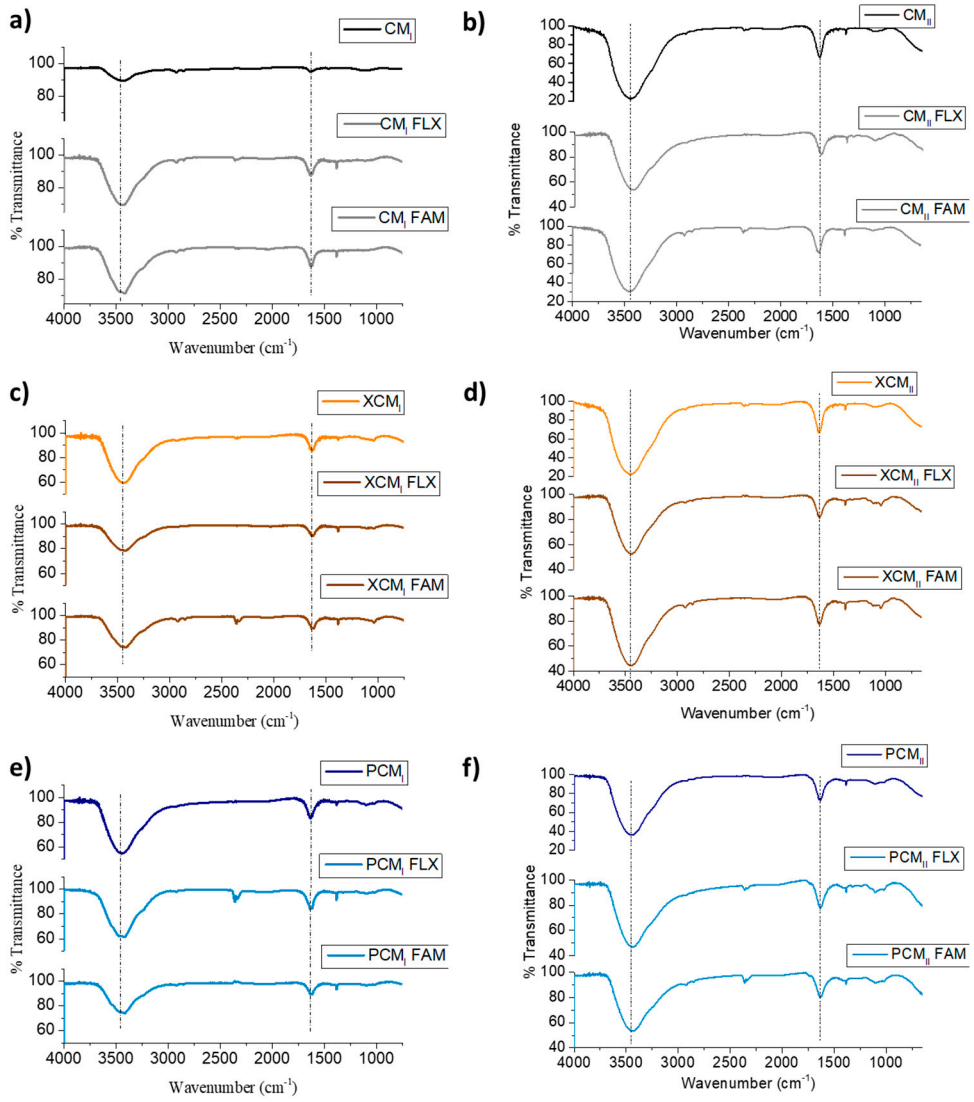

Figure 2. FTIR spectra of (**a**) CM_I, (**b**) CM_{II}, (**c**) XCM_I, (**d**) XCM_{II}, (**e**) PCM_I, and (**f**) PCM_{II} before and after adsorption of FLX and FAM.

3.2. Adsorption Performance

The adsorption performance of FLX and FAM on the prepared nanocomposites is depicted in Figure 3. High removal percentages reaching 80–95% were obtained with pectin-based and AC-based composites. Generally, it is clearly shown that the composites synthesized by route II; CM_{II} and PCM_{II}, mostly exhibited a non-significant difference in percent removal for FLX ($p > 0.05$), compared to those prepared using route I (i.e., CM_I and PCM_I), with the exception of XCM_I, which gave a percent removal increase of 27.6% ($p < 0.05$) compared to XCM_{II}. However, for FAM, only CM_I and CM_{II} showed non-significant or comparable percent removal values ($p > 0.05$), while PCM_{II} exhibited a lower percent removal than PCM_I by 10.8% ($p < 0.05$), and XCM_{II} showed a higher percent removal than XCM_I by 30.3% ($p < 0.05$). Though the removal percentages of FAM are apparently higher than those of FLX with CM_{II}, XCM_{II} and PCM_{II}, only XCM_{II} showed a significantly higher percent removal for FAM than FLX ($p < 0.05$), unlike CM_{II} and PCM_{II} ($p > 0.05$). FLX was bound more favorably to XCM_I than XCM_{II}, since the xylan that coats the surface of XCM_I provides polar functional groups that can capture FLX. However, FAM was bound more favorably to XCM_{II} than XCM_I since XCM_{II} surfaces are dominated by hydrophobic centers that could adsorb the hydrophobic drug, which also explains the higher adsorption of FAM relative to FLX on the former nanocomposite. As

for PCM_I, the pectin dominating its surface provides both the polar functional groups and the hydrophobicity (being a methylated and galacturonated polymer) which can remove FAM with higher efficiency than PCM_{II}.

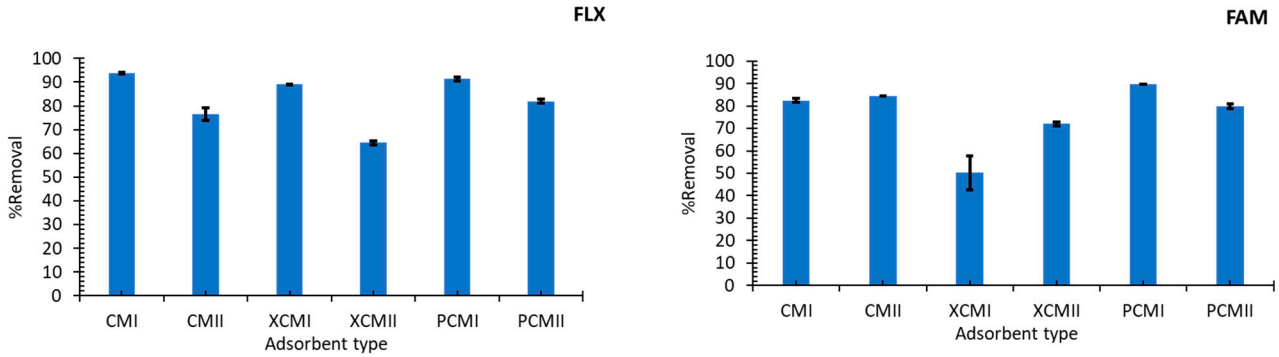

(**a**) (**b**)

Figure 3. Percent removal of (**a**) FLX and (**b**) FAM on the prepared nanocomposites at an initial concentration of 25 ppm, adsorbent dose of 0.67 g/L, and pH 7.35. Values expressed as mean ± SD (n = 2).

3.3. Mechanism of Adsorption

According to the zeta potential measurements at the working pH of 7.35 (Table 1), all nanocomposites are negatively charged and hence can interact with the positively charged FLX (pK_a 9.8) or FAM (pK_a 7.95) via electrostatic interactions. The mechanism of adsorption of FLX and FAM on the nanocomposites has also been investigated through FTIR measurements before and after adsorption as depicted in Figure 2. In composites prepared via route I, CM_I showed an increase in the intensity of OH and C=O bands after FLX or FAM adsorption. However, XCM_I exhibited a decrease in the intensities of these bands. PCM_I showed a shift and change in the intensity of the OH band after FLX adsorption, while a shift in this band and the C=O band along with an intensity change was recorded after FAM adsorption. For the composites synthesized by route II, CM_{II}, XCM_{II} and PCM_{II} exhibited a clear change in the intensity of the OH and C=O bands after FLX or FAM adsorption. These results manifest the role of hydroxyl and carboxylic acid groups in the adsorption of FLX and FAM from aqueous solutions possibly through electrostatic forces or hydrogen bonding. This does not negate the possibility of there being hydrophobic interactions as well.

4. Conclusions

Successful preparation of biopolymer-incorporated activated charcoal/magnetite nanocomposites was achieved via two different synthesis routes I and II. Nanocomposites prepared via synthesis route I had the biopolymer as the dominant coating on the surface, while those prepared via synthesis route II had the activated charcoal on the surface. Regarding removal efficiency, XCM nanocomposites prepared via synthesis route I exhibited better removal percentage of FLX and less removal of FAM when compared to their corresponding nanocomposites prepared via synthesis route II. Adsorption occurred mainly via electrostatic attractions alongside other possible mechanisms of hydrophobic interactions and hydrogen bonding.

Author Contributions: Performing the experiments, writing and figure design, H.H.F.; writing and supervision, M.N.; writing, data curation and supervision, M.M.H.E.-S. All authors have read and agreed to the published version of the manuscript.

Funding: This research was funded by The American University in Cairo PhD grant, and USAID ASHA grant: AID-ASHA-G-17-00010.

Institutional Review Board Statement: Not applicable.

Informed Consent Statement: Not applicable.

Data Availability Statement: Not applicable.

Conflicts of Interest: The authors declare no conflict of interest.

References

1. Rathi, B.S.; Kumar, P.S.; Show, P.-L. A review on effective removal of emerging contaminants from aquatic systems: Current trends and scope for further research. *J. Hazard. Mater.* **2021**, *409*, 124413. [CrossRef] [PubMed]
2. Lam, M.W.; Young, C.J.; Mabury, S.A. Aqueous Photochemical Reaction Kinetics and Transformations of Fluoxetine. *Environ. Sci. Technol.* **2005**, *39*, 513–522. [CrossRef] [PubMed]
3. Matsuo, H.; Sakamoto, H.; Arizono, K.; Shinohara, R. Behavior of Pharmaceuticals in Waste Water Treatment Plant in Japan. *Bull. Environ. Contam. Toxicol.* **2011**, *87*, 31–35. [CrossRef] [PubMed]
4. Brooks, B.W.; Foran, C.M.; Richards, S.M.; Weston, J.; Turner, P.K.; Stanley, J.K.; Solomon, K.R.; Slattery, M.; La Point, T.W. Aquatic ecotoxicology of fluoxetine. *Toxicol. Lett.* **2003**, *142*, 169–183. [CrossRef] [PubMed]
5. Afsa, S.; Hamden, K.; Martin, P.A.L.; Ben Mansour, H. Occurrence of 40 pharmaceutically active compounds in hospital and urban wastewaters and their contribution to Mahdia coastal seawater contamination. *Environ. Sci. Pollut. Res.* **2020**, *27*, 1941–1955. [CrossRef]
6. Chai, W.S.; Cheun, J.Y.; Kumar, P.S.; Mubashir, M.; Majeed, Z.; Banat, F.; Ho, S.-H.; Show, P.L. A review on conventional and novel materials towards heavy metal adsorption in wastewater treatment application. *J. Clean. Prod.* **2021**, *296*, 126589. [CrossRef]
7. Moosavi, S.; Lai, C.W.; Gan, S.; Zamiri, G.; Pivehzhani, O.A.; Johan, M.R. Application of Efficient Magnetic Particles and Activated Carbon for Dye Removal from Wastewater. *ACS Omega* **2020**, *5*, 20684–20697. [CrossRef] [PubMed]
8. Silva, B.; Martins, M.; Rosca, M.; Rocha, V.; Lago, A.; Neves, I.C.; Tavares, T. Waste-based biosorbents as cost-effective alternatives to commercial adsorbents for the retention of fluoxetine from water. *Sep. Purif. Technol.* **2020**, *235*, 116139. [CrossRef]
9. Rad, T.S.; Khataee, A.; Kayan, B.; Kalderis, D.; Akay, S. Synthesis of pumice-TiO2 nanoflakes for sonocatalytic degradation of famotidine. *J. Clean. Prod.* **2018**, *202*, 853–862. [CrossRef]
10. Omraei, M.; Esfandian, H.; Katal, R.; Ghorbani, M. Study of the removal of Zn(II) from aqueous solution using polypyrrole nanocomposite. *Desalination* **2011**, *271*, 248–256. [CrossRef]
11. Buvaneswari, K.; Singanan, M. Review on scanning electron microscope analysis and adsorption properties of different activated carbon materials. *Mater. Today Proc.* **2020**, in press. [CrossRef]
12. Sharma, K.; Khaire, K.C.; Thakur, A.; Moholkar, V.S.; Goyal, A. Acacia Xylan as a Substitute for Commercially Available Xylan and Its Application in the Production of Xylooligosaccharides. *ACS Omega* **2020**, *5*, 13729–13738. [CrossRef] [PubMed]
13. Li, F.T.; Yang, H.; Zhao, Y.; Xu, R. Novel modified pectin for heavy metal adsorption. *Chin. Chem. Lett.* **2007**, *18*, 325–328. [CrossRef]
14. Alcaraz, L.; Fernández, A.L.; García-Díaz, I.; López, F.A. Preparation and characterization of activated carbons from winemaking wastes and their adsorption of methylene blue. *Adsorpt. Sci. Technol.* **2018**, *36*, 1331–1351. [CrossRef]
15. Zhang, L.; He, R.; Gu, H.-C. Oleic acid coating on the monodisperse magnetite nanoparticles. *Appl. Surf. Sci.* **2006**, *253*, 2611–2617. [CrossRef]
16. Illés, E.; Tombácz, E. The role of variable surface charge and surface complexation in the adsorption of humic acid on magnetite. *Colloids Surf. A Physicochem. Eng. Asp.* **2003**, *230*, 99–109. [CrossRef]